Available online at www.sciencedirect.com
SCIENCE DIRECT®
C. R. Chimie 7 (2004) 1135–1140
COMPTES RENDUS CHIMIE
http://france.elsevier.com/direct/CRAS2C/

Full paper / Mémoire

In situ high temperature NMR and EXAFS experiments in rare-earth fluoride molten salts

Anne-Laure Rollet [a,*], Catherine Bessada [a], Aïdar Rakhmatoulline [a], Yannick Auger [a], Philippe Melin [a], Marc Gailhanou [b], Dominique Thiaudière [a]

[a] *CNRS–CRMHT, 1D, av. de la Recherche-Scientifique, 45071 Orléans cedex 2, France*
[b] *LURE, bât. 209D, université Paris-Sud, 91898 Orsay cedex, France*

Received 18 September 2003; accepted after revision 10 February 2004

Available online 13 October 2004

Abstract

The local structure in molten YF_3–LiF and LaF_3–LiF binaries has been investigated by NMR and EXAFS spectroscopy. For YF_3–LiF, the high-temperature ^{19}F and ^{7}Li NMR spectra have been recorded in situ in the molten state for compositions ranging from pure LiF to pure YF_3. The LaF_3–LiF system has been studied by ^{19}F and ^{139}La NMR and EXAFS spectroscopy at the LIII edge of La. The local environment around the La^{3+} in the molten state does not depend on the composition, while ^{19}F chemical shift evolution confirms the progressive formation of bridged species. ***To cite this article: A.-L. Rollet et al., C. R. Chimie 7 (2004)***.

Résumé

Étude in situ par spectroscopies RMN et EXAFS à haute température de fluorures de terres rares fondus. La structure locale des mélanges fondus YF_3–LiF et LaF_3–LiF a été étudiée par spectroscopies RMN et EXAFS à haute température. Pour le système YF_3–LiF, les spectres RMN à haute température de ^{19}F et ^{7}Li ont été enregistrés in situ dans le liquide pour différentes compositions variant de LiF pur à YF_3 pur. Le système LaF_3–LiF a été étudié par RMN de ^{19}F et ^{139}La, et par EXAFS au seuil LIII du lanthane. L'environnement autour du La^{3+} à l'état fondu ne dépend pas de la composition, alors que les évolutions du déplacement chimique du fluor confirment la formation progressive d'espèces pontantes. ***Pour citer cet article : A.-L. Rollet et al., C. R. Chimie 7 (2004)***.

Keywords: Lanthanide trifluorides; Molten salts; High temperature; NMR; EXAFS

Mots clés : Fluorures de lanthanides ; Sels fondus ; Haute température ; RMN ; EXAFS

* Corresponding author.
E-mail address: rollet@cnrs-orleans.fr (A.-L. Rollet).

1631-0748/$ - see front matter © 2004 Académie des sciences. Published by Elsevier SAS. All rights reserved.
doi:10.1016/j.crci.2004.02.021

1. Introduction

Manipulation hindrances caused by relatively elevated melting points (300–1500 °C) and high corrosiveness have generated scarcity in experimental data for molten fluoride salts. However, there is no doubt that they represent a rich realm of fundamental research and industrial applications because of their physical and chemical properties [1]: high thermal conductivity and capacity, moderate viscosity, high electrical conductivity, mutual miscibility, wide range of thermochemical and electrochemical stability, low dielectric constants, good non-aqueous solvents, hygroscopicity... Their electrochemical and solvent properties have given rise to many applications in the field of electrolytic processes in metallurgy, such as the production of aluminium [2] or for refractory-metal deposition. Moreover, they are used in the Molten Salt Nuclear Reactor (MSR) [3,4]. In the latter case, radioactive elements are dissolved in a molten salt and extraction of fission product is continuously performed by using electrochemical processes in a secondary circuit. The molten salt systems used in MSR consist of a solvent composed by alkali fluorides (LiF, NaF) plus beryllium fluoride and the lanthanide and actinide fluorides. Owing to the mutual miscibility of molten salts, no precipitation phenomena occur, whatever the element and the composition. This is of crucial importance in nuclear reactors, where no local deposition of any elements can be accepted for safety reasons.

Given the fact that most of the studies concerning these kinds of systems are focused on thermodynamic aspects, much work is due to be carried out [5,6]. Thus phase diagrams of LiF–LnF_3 systems are of two kinds: simple from lanthanum to samarium, with an eutectic point around 20 mol% of LnF_3, more complex from europium to lutetium, with several solid phases and two eutectic points (from erbium). As regards structure of the molten lanthanide fluorides, nature of neighbours, coordination and distances around the cation, is still matter of debate. So far, the main spectroscopic results have been carried out by Raman spectroscopy [7]. For instance, in molten KF–LnF_3 binary systems rich in KF, the lanthanides appear to be in an octahedral configuration LnF_6^{3-} for all the lanthanide systems studied. This structure is preserved in melts up to 1000 °C and for all the compositions studied, i.e. from 0 to 50 mol% of LnF_3. For compositions rich in LnF_3, the octahedra are bridged by fluorine. In addition, the LnF_6^{3-} complexes are more stable than the other halides lanthanides LnX_6^{3-} (X = Cl, Br, I). In this paper, we intend to present structural data obtained by two complementary spectroscopic techniques: Extended X-ray Absorption Fine Structure (EXAFS) and Nuclear Magnetic Resonance (NMR). In order to adjust these techniques to high-temperature molten fluorides, we had to make specific developments of the different experimental devices. In the case of NMR, the device was developed in the CRMHT laboratory few years ago [8], and has been successfully used in the study of molten alkali fluoroaluminates [9]. In the case of EXAFS, we have built a new cell compatible with the molten fluorides and X-ray spectroscopy requirements. To our knowledge, it is the first time that EXAFS experiments have been carried out on molten lanthanide fluorides at a temperature close to 1000 °C.

In this publication, two fluoride lanthanide binary systems have been studied: LaF_3–LiF, and YF_3–LiF. Interest of studying these two systems also emerges from the fact that La is representative of the lightest lanthanides, whereas Y is representative of the heaviest. Furthermore, the NMR study of lanthanide trifluorides is particularly difficult, because most of them are paramagnetic, generally preventing any NMR observation of all the surrounding nuclei. Fortunately it is not the case for La^{3+} and Y^{3+}, which are diamagnetic and observable by NMR. The combination of multinuclear NMR and EXAFS experiments may be useful tool in structural description of melts.

2. Experimental

The fluoride salts (purity 99.99%) were purchased from Aldrich. The appropriate quantities of binary mixtures were weighed and then filled into NMR and EXAFS cells in a glovebox under dried argon in order to avoid H_2O and O_2 contamination of the samples. The composition of YF_3–LiF ranged from 0 to 100 mol% and LaF_3–LiF composition from 0 to 60%.

The NMR spectra were recorded using a Bruker DSX 400 NMR and DSX 300 spectrometer, operating at 9.40 and 7.04 T, respectively. In situ high-temperature NMR static spectra were obtained by using the previously described [9] high-temperature laser-heated system developed at the CRMHT–CNRS

in Orleans (France). In these highly corrosive systems, the temperature cannot be measured inside the sample during the experiment. In the case of NMR device, a calibration is previously performed: a thermocouple is put in a BN crucible filled with a BN powder and the temperature is measured as a function of the laser power. The spectra presented here were collected about 20 K above the corresponding melting points. The temperature is not given precisely for each experiment, as we noticed that the mean local structure is not affected by the melt temperature (NMR and EXAFS results not detailed in this note). The various spectra were acquired using a single-pulse sequence, with $\pi/12$ pulses, a recycle delay of 0.5 s, and 8 to 128 accumulations. Samples, 50 to 65 mg, were put in a boron-nitride (BN) crucible tightly closed by a screw cap. The samples were heated directly up to melts. ^{19}F solid-state MAS NMR spectra have been obtained at room temperature on quenched samples after HT NMR experiments. The solid-state NMR data were collected with the same spectrometer (9.4 T) using a 2.5 mm MAS probe for a 35 kHz spinning rate. The acquisition parameters were chosen to optimise the resolution: short pulse lengths (0.5 μs), recycle times of 1 to 5 s.

The EXAFS experiments were carried out on H10 beam line [10] at LURE/DCI ('Laboratoire pour l'utilisation du rayonnement électromagnétique', Orsay, France). This beam line is mainly dedicated to X-ray diffraction and X-ray absorption measurements in a tunable energy range (4–20 keV). The energy was ranging from 5.4 to 5.85 keV (LIII edge of La: 5.48 keV). The white X-ray beam is collimated by a first mirror placed before the monochromator and the monochromated beam is given by a fixed-exit two-crystal Si(111). The X-ray beam is focused from the second crystal in the horizontal plane and from the second mirror in the vertical one. Both mirrors are coated with rhodium and ensure the harmonic rejection. The cell was made by two excavated plates of pyrolitic boron nitride maintained fixed by screws. The cell was placed in a tubular furnace under vacuum. Due to the geometry of the furnace, in situ EXAFS spectra were recorded in a transmission mode using Si photodiode as detector placed behind a furnace. The heating rate was 10 °C min^{-1} up to 1000 °C. The distances reported in this paper are not exactly the real distances but shifted about –0.5 Å, due to a problem of phase correction. The data analysis has been performed using the WINXAS software.

3. Results and discussion

3.1. NMR

The ^{19}F NMR spectra in molten and solid LiF–YF_3 are presented in Fig. 1 for compositions ranging from 0 to 100 mol% of YF_3. The peak position of pure LiF, $LiYF_4$, and YF_3 melts is shifted to higher ppm values compared with the corresponding solids. This effect is greater for YF_3 than for $LiYF_4$ and LiF. This finding shows clearly that the electronic environment of fluorine has a weaker screen effect in the melt than in the solid; the modification of the electronic environment is stronger in YF_3. The measured chemical shift provides information on the local environment around the observed nucleus and depends on the nature and the number of neighbours. The chemical shift range depends also on the nucleus itself ranging from some ppm for proton to some thousands of ppm for platinum. In our particular cases, the δ range is about few ppm for ^{7}Li, while for ^{19}F and ^{139}La, it is about several hundreds of ppm [11].

In melts, all contributions emerge in a single line as a result of rapid exchange between the different species, at the timescale of NMR. Nevertheless, the experimental position is the weighed average of the position of each species present in melts. The position of

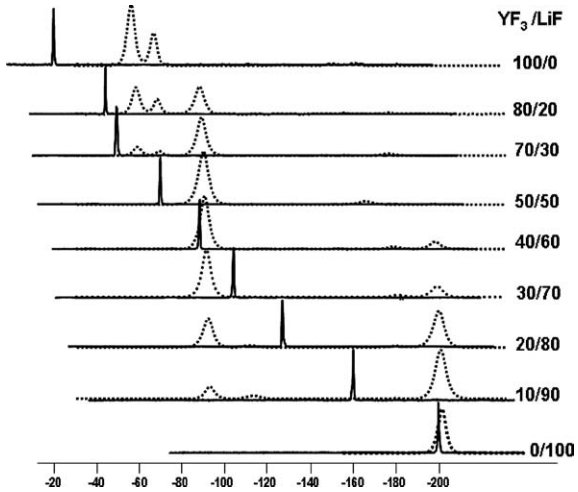

Fig. 1. ^{19}F NMR spectra in YF_3–LiF system for various compositions. The high-temperature ^{19}F spectra in the melts are in black lines and the MAS ^{19}F spectra in solidified samples are in dashed lines. The spectra of molten and solid state are superimposed to help the visualization of the chemical shift variation, but the relative intensities cannot be compared.

this peak is progressively shifted toward higher δ value, but is not modified by the temperature of the melt (results not presented here). This variation of the ^{19}F and ^{7}Li chemical shifts is represented versus the composition in Fig. 2. The ^{19}F chemical shift monotonously increases when the YF_3 amount is increased. A variation corresponding to the particular variation of the melting temperature in the phase diagram, especially around the eutectic points, could have been expected. Two explanations can be put forward: the local structure is continuously and monotonously changed with the melt composition, or at least another complex arises as the composition becomes richer in YF_3. At the same time, ^{7}Li chemical shift remains the same whatever the composition, thus supporting the second hypothesis. Unfortunately, the chemical shift range of ^{7}Li is very weak and this result does not allow us to definitely conclude.

The ^{19}F MAS spectra of the solidified samples after high-temperature experiments are shown also in Fig. 1. Starting from pure LiF with a single peak at –200 ppm, we notice with YF_3 addition the emergence of a second peak at –90 ppm assignable to $LiYF_4$ [12]. Exceeding 50 mol% YF_3, the LiF peak vanishes while the two peaks corresponding to the two different fluorine sites of YF_3 [13] appear at –56 and –67 ppm. The comparison of the peak positions in the melts and in the solids suggests that several species in rapid exchange are present in the melts. These fluorine species are those existing in pure LiF and $LiYF_4$ from 0 to 50 mol%, and those in pure $LiYF_4$ and YF_3 from 50 to 100 mol%.

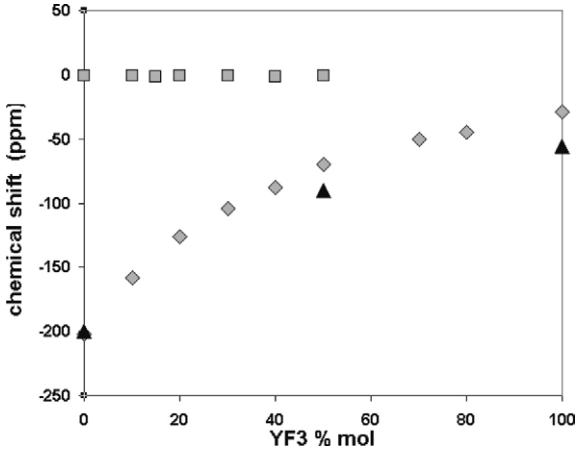

Fig. 2. Variation of the ^{19}F (grey diamond) and ^{7}Li chemical shifts (grey square) in melts and ^{19}F in solidified samples (black triangle) versus YF_3 mol%.

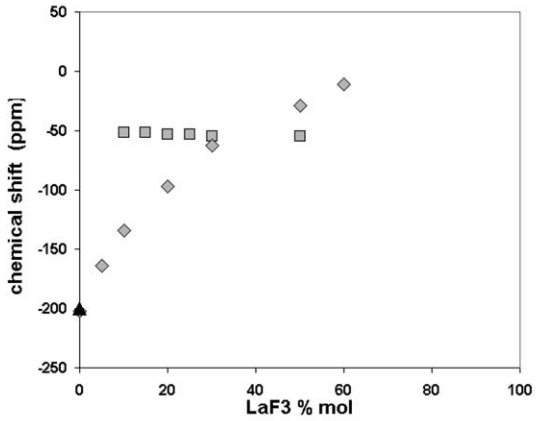

Fig. 3. Variation of the ^{19}F (grey diamond) and ^{139}La chemical shifts in melts (grey square) and ^{19}F in solidified samples (black triangle) versus LaF_3 mol%.

This evolution signs the progressive modification of the fluorine environment from free fluorine in LiF towards YF_x^{3-x} configuration. We can explain this evolution with an increase in the bridging fluorines in the melt for LnF_3 addition.

A similar study has been carried out on the system LaF_3–LiF. The ^{19}F and ^{139}La NMR findings are illustrated in Fig. 3 as a function of the LaF_3 mol%. Like YF_3–LiF system, the ^{19}F chemical shift increases monotonously as LaF_3 quantity is increased, without any intricate evolution at eutectics. Moreover, no variation of the ^{139}La chemical shift occurs over the whole composition range. This behaviour is the same as for ^{7}Li, but, in the case of ^{139}La, it is perfectly relevant and indicates a non-variation of the La environment. Indeed, the chemical shift range of ^{139}La is several hundreds ppm, resulting in a great sensitivity to the nucleus surrounding.

The information supplied by the ^{19}F, ^{7}Li and ^{139}La NMR data confirms the existence of more than one environment around the fluorine atoms. Their proportion depends on the composition, while the lanthanum environment remains unchanged.

3.2. EXAFS

Since few literature data concern chloride [14] and bromide molten salts [15,16], this study represents, to our knowledge, the first attempt to investigate molten fluoride salts by EXAFS spectroscopy. The experimental device had to be especially developed for these

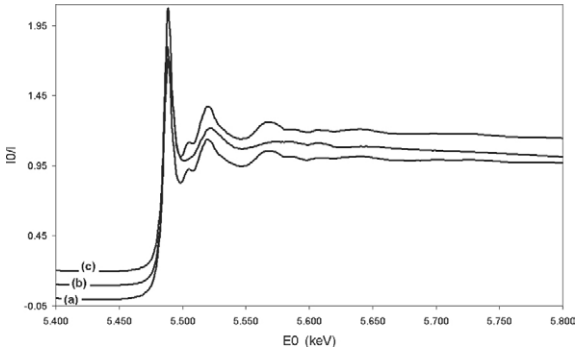

Fig. 4. The X-ray LIII edge lanthanum absorption spectra in LaF_3 solid (a), in molten LiF–LaF_3 20–80 mol% (b) and in the solid formed by cooling (20 °C min^{-1}) the molten LiF–LaF_3 20–80 mol% system (c).

highly corrosive and volatile fluoride melts. The high stability achieved (no evaporation or no interaction of chemicals and no corrosion of the cell...) allowed us to collect data during several hours. The absorption spectra are presented in Fig. 4 for solid LaF_3, 20–80 mol% LiF–LaF_3 molten mixture and the corresponding solid formed on cooling at a rate of 20 °C min^{-1}. The usual features of the liquid compared with those of the corresponding solid are observed here: the oscillations after the absorption edge are damped more rapidly. Another striking feature is the loss of the oscillation located at 5.506 keV in the molten state. This oscillation occurs in the XANES region (up to 50 eV above the absorption edge), and provides information about the electronic structure of the absorbent atom. The loss of the 5.506 keV oscillation indicates a modification in the electronic state of the La atom.

Radial structure function for the LaF_3 solid, the melt and the solid formed after cooling of the 10–90 **(a)** and 20–80 mol% **(b)** LaF_3–LiF molten mixtures are presented in Fig. 5, where the radial structure function is displayed. In the LaF_3 solid, two peaks are visible: one around 2 Å and a much smaller one around 3.8 Å. The first peak can be ascribed to the fluorine neighbours, and the second one to the lanthanum environment, the lithium being too light to be detected. In the melt, beyond the first peak around 2 Å, no significant peak was found. Indeed, because of high-temperature effects, the displacement of the atoms leads to an information loss for longer distances. Moreover, the shape of the peaks in the solid is symmetric, contrary to the melt, where they become asymmetric. EXAFS studies of other melts have already shown such a phenomenon

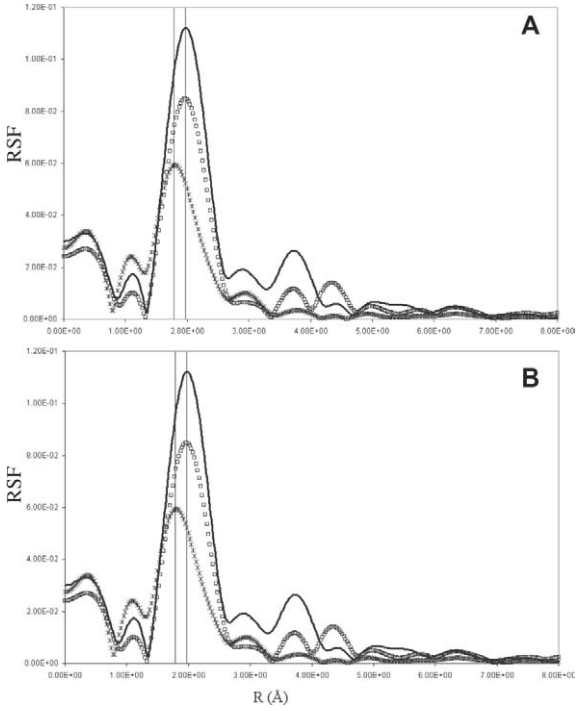

Fig. 5. Radial structure function of Lanthanum in solid LaF_3 (black line), in molten state (black cross) and in the solid formed on cooling (20°/min^{-1}) (white square) for **(a)** LaF_3–LiF 10–90 mol% and **(b)** LaF_3–LiF 20–80 mol%.

[14,17–19]. For YCl_3 and YBr_3 [14], it has been ascribed to an anharmonic vibration effect in the molten state. In our study, the La–F distance in this first shell is decreased in all melts in comparison with their corresponding solids, contrary to the YCl_3 and YBr_3 systems, where a very slight increase occurs [14]. This increase is all the more pronounced since the YX_3 amount in the melt is large. Nevertheless, in both YX_3 (X = Br and Cl) and LaF_3 systems, the distance Ln–F seems not to be influenced by the composition of the melt, which is in agreement with our NMR results. Similar results have also been observed in Raman spectra [20], which show very weak changes with LaF_3 amount in the LaF_3–KF system in the 0–40 mol% LaF_3 range.

4. Conclusion

The local structure of molten YF_3–LiF and LaF_3–LiF binary systems has been studied using NMR and EXAFS techniques. These two different systems are

characterized by the same structural evolution, whereas they exhibit rather different phase diagrams. The results indicate the presence of different complexes, whose proportion is determined by the composition of the melt. These complexes remain unchanged when the composition is changed, particularly the distance lanthanide–fluorine of the first shell of neighbours around the lanthanide is kept constant.

Acknowledgements

The authors thank the LURE for providing synchrotron source. They are indebted to GDR PRACTIS for the financial help for EXAFS cells development. The authors acknowledge Christophe DenAuwer for fruitful discussions and his help on EXAFS data treatment.

References

[1] D.G. Lovering, R.J. Gale, Molten Salt Techniques, Plenum Press, New York and London, 1987.
[2] K. Grojtheim, C. Krohn, M. Malinovsky, K. Matiasovsky, J. Thonstad, Aluminium electrolysis, Fundamentals of the Hall-Heroult process, 2nd Ed., Aluminium-Verlag, Düsseldorf, 1982.
[3] A. Nuttin, PhD thesis, University Joseph-Fourier, Grenoble, France, ISN0288, 2002.
[4] P.N. Haubenreich, J.R. Engel, Nucl. Appl. Technol. 8 (1970) 118.
[5] B.P. Sobolev, The Rare Earth Trifluorides part 1, Institut d'Estudis Catalans, Barcelona, 2000.
[6] B.P. Sobolev, The Rare Earth Trifluorides part 2, Institut d'Estudis Catalans, Barcelona, 2001.
[7] V. Dracopoulos, B. Gilbert, B. Borrensen, G.M. Photiadis, G.N. Papatheodorou, J. Chem. Soc. Faraday Trans. 93 (1997) 3081.
[8] V. Lacassagne, C. Bessada, B. Ollivier, D. Massiot, J.-P.C. Coutures, C.R. Acad. Sci. Paris, Ser. IIb 325 (1997) 91.
[9] V. Lacassagne, C. Bessada, P. Florian, S.B. Bouvet, Ollivier, J.-P.C. Coutures, D. Massiot, J. Phys. Chem. B 106 (2002) 1862.
[10] M. Gailhanou, J.-M. Dubuisson, M. Ribbens, L. Roussier, D. Bétaille, C. Créoff, M. Lemonnier, J. Denoyer, C. Bouillot, A. Jucha, A. Lena, M. Idir, M. Bessière, D. Thiaudière, L. Hennet, C. Landron, J.-P. Coutures, Nucl. Instrum. Meth. A 467–468 (2001) 745.
[11] R.K. Harris, B.E. Mann (Eds.), NMR and the periodic table, Academic Press, London, 1978.
[12] E. Garcia, R.R. Ryan, Acta Crystallogr. C 41 (1993) 2053.
[13] A.K. Cheetham, N. Norman, Acta Chem. Scand. A 28 (1974) 55.
[14] Y. Okamoto, M. Akabori, H. Motohashi, H. Shiwaku, T. Ogawa, J. Synchrotron Rad. 8 (2001) 1191.
[15] R.A. La Violette, J.-L. Budzien, F.H. Stillinger, J. Chem. Phys. 112 (2000) 8072.
[16] A. Di Cicco, M. Minicucci, A. Filipponi, Phys. Rev. Lett. 78 (1997) 460.
[17] C. Landron, L. Hennet, J.-P. Coutures, M. Gailhanou, M. Gramond, J.-F. Berar, Europhys. Lett. 44 (1998) 429.
[18] E.A. Stern, P. Livins, Z. Zhang, Phys. Rev. B 43 (1991) 8850.
[19] DiCicco, M. Minicucci, A. Filiponi, Phys. Rev. Lett. 78 (1997) 460.
[20] V. Dracopoulos, B. Gilbert, G.N. Papatheodorou, J. Chem. Soc., Faraday Trans. 94 (1998) 2601.